Chromosome-scale and haplotype-resolved genome assembly of a tetraploid potato cultivar

Hequan Sun[1,2,†], Wen-Biao Jiao[1,2,3,4,†], José A. Campoy[2], Kristin Krause[1,2], Manish Goel[1,2], Kat Folz-Donahue[5], Christian Kukat[5], Bruno Huettel[6], and Korbinian Schneeberger[1,2,*]

[1]Faculty of Biology, LMU Munich, Großhaderner Str. 2, 82152 Planegg-Martinsried, Germany

[2]Department of Chromosome Biology, Max Planck Institute for Plant Breeding Research, Carl-von-Linné-Weg 10, 50829 Cologne, Germany

[3]Key Laboratory of Horticultural Plant Biology (Ministry of Education), Huazhong Agricultural University, 430070 Wuhan, China

[4]College of Informatics, Huazhong Agricultural University, 430070 Wuhan, China

[5]FACS & Imaging Core Facility, Max Planck Institute for Biology of Ageing, 50931 Cologne, Germany

[6]Max Planck-Genome-center Cologne, Carl-von-Linné-Weg 10, 50829 Cologne, Germany

[†]These authors contributed equally

*Corresponding author. Email: schneeberger@mpipz.mpg.de

Abstract

Potato is the most important tuber crop in the world. However, separate reconstruction of the four haplotypes of its autotetraploid genome remained an unsolved challenge. Here, we report the 3.1 Gb haplotype-resolved (at 99.6% precision), chromosome-scale assembly of the potato cultivar 'Otava' using high-quality long reads coupled with single-cell sequencing of 717 pollen genomes and Hi-C data. Unexpectedly, almost 50% of the genome were found to be identical-by-descent due to recent inbreeding, which contrasted by highly abundant structural rearrangements involving around 20% of the genome. Among 38,214 genes, only 54% were present in four haplotypes with an average of 3.2 copies per gene. Analyzing the leaf transcriptome as example, we found that 11% of the genes featured differently expressed alleles in at least one of the haplotypes, of which 25% are likely regulated through allele-specific DNA methylation. Our work sheds light on the recent breeding history of potato, the functional organization of its tetraploid genome and has the potential to strengthen the future of genomics-assisted breeding.

Potato (*Solanum tuberosum*) is by far the most important tuber crop and is among the five most produced crops in the world. Globally more than 350 billion kilograms of potato are produced per year with an increasing trend particularly in developing countries in Asia[1]. Despite the social and economic importance, the breeding success of potato remained low over the past decades due to its heterozygous, autotetraploid genome and the high levels of inbreeding depression, which challenge usual breeding strategies commonly applied to inbred, diploid crops[2,3].

A fundamental tool for modern breeding is the availability of reference sequences. The reference sequence for potato was generated from a double haploid plant, *DM1-3 516 R44* (*DM*), and was initially published in 2011[4] and continuously improved over the past years including a recent update based on long read sequencing[5,6]. Another major advancement in potato genomics was the recent assembly of a heterozygous diploid potato, *RH89-039-16*

45 (*RH*)[7]. This haplotype-resolved genome was generated from a variety of different sequencing
46 technologies and phase information from a genetic map derived from selfed progeny.
47 However, as of now, there is no haplotype-resolved assembly of a tetraploid potato
48 cultivar available nor there is a straightforward method that would enable the assembly of the
49 individual haplotypes of a tetraploid genome. The latest methods for haplotype phasing include
50 the separation of sequencing reads based on the differences between the parental genomes[8]
51 or based on haplotype information derived from gamete[9-12] or offspring genomes[7,13]. Similarly,
52 chromosome conformation capture sequencing (e.g., Hi-C) can help to resolve haplotypes
53 during or before the assembly[14-18] and has been applied to polyploids already[15-17]. However,
54 even though straightforward in its application, chromosome conformation capture sequencing
55 can lead to haplotype switch errors, and requires additional efforts such genetic maps for
56 correction[7,9,18].

57 **Genome assembly of a tetraploid potato**

58 We generated an assembly of the autotetraploid genome of *S. tuberosum* 'Otava' using
59 high-quality long PacBio HiFi reads (30x per haplotype) using *hifiasm*[19] (Fig. 1; Data S1; Fig.
60 S1-2; Methods). The initial assembly consisted of 6,366 contigs with an N50 of 2.1 Mb (Fig.
61 S3). While the total assembly size of 2.2 Gb was much larger than the estimated haploid
62 genome size of ~840 Mb, it accounted only for ~65% of the tetraploid genome size (Fig. S2)
63 indicating that one third of the genome collapsed during the assembly. A sequencing depth
64 histogram across the contigs featured four distinct peaks, which originated from regions with
65 either one, two, three, or four (collapsed) haplotype(s) (Fig. 1b). While most of the contigs
66 represented only one haplotype (referred to as *haplotigs*) and accounted for 1.5 Gb (68%) of
67 the assembly, contigs representing two, three or even four collapsed haplotypes (referred to
68 as *diplotigs*, *triplotigs* or *tetraplotigs*) still made up 470 Mb (21%), 173 Mb (8%) or 43 Mb (2%).
69 Regions with even higher coverages were virtually absent (9.4 Mb, 0.4%).
70 As there is no straight forward solution to untangle collapsed contigs after the assembly,
71 we restarted the genome assembly, but this time based on four separated read sets each
72 derived from one of the four haplotypes. In diploids, such a read separation prior to the

assembly can be performed by sorting the reads according to their similarity to the parental genomes (trio binning)[8]. But as autotetraploid individuals inherit two haplotypes through both the maternal and paternal lineages, this cannot be applied for autotetraploid genomes. Alternatively, the reads can also be separated using the haplotypes found in gamete genomes (gamete binning)[9]. While this is straightforward with haploid gametes from diploid individuals, tetraploid potato develops diploid gametes, which again does not separate individual haplotypes. However, as the pairing of the two haplotypes in a diploid gamete is random in potato, we speculated that it might be possible to gain information on individual haplotypes (and thus to separate the reads into four distinct sets) if we sequence a sufficient number of diploid gametes.

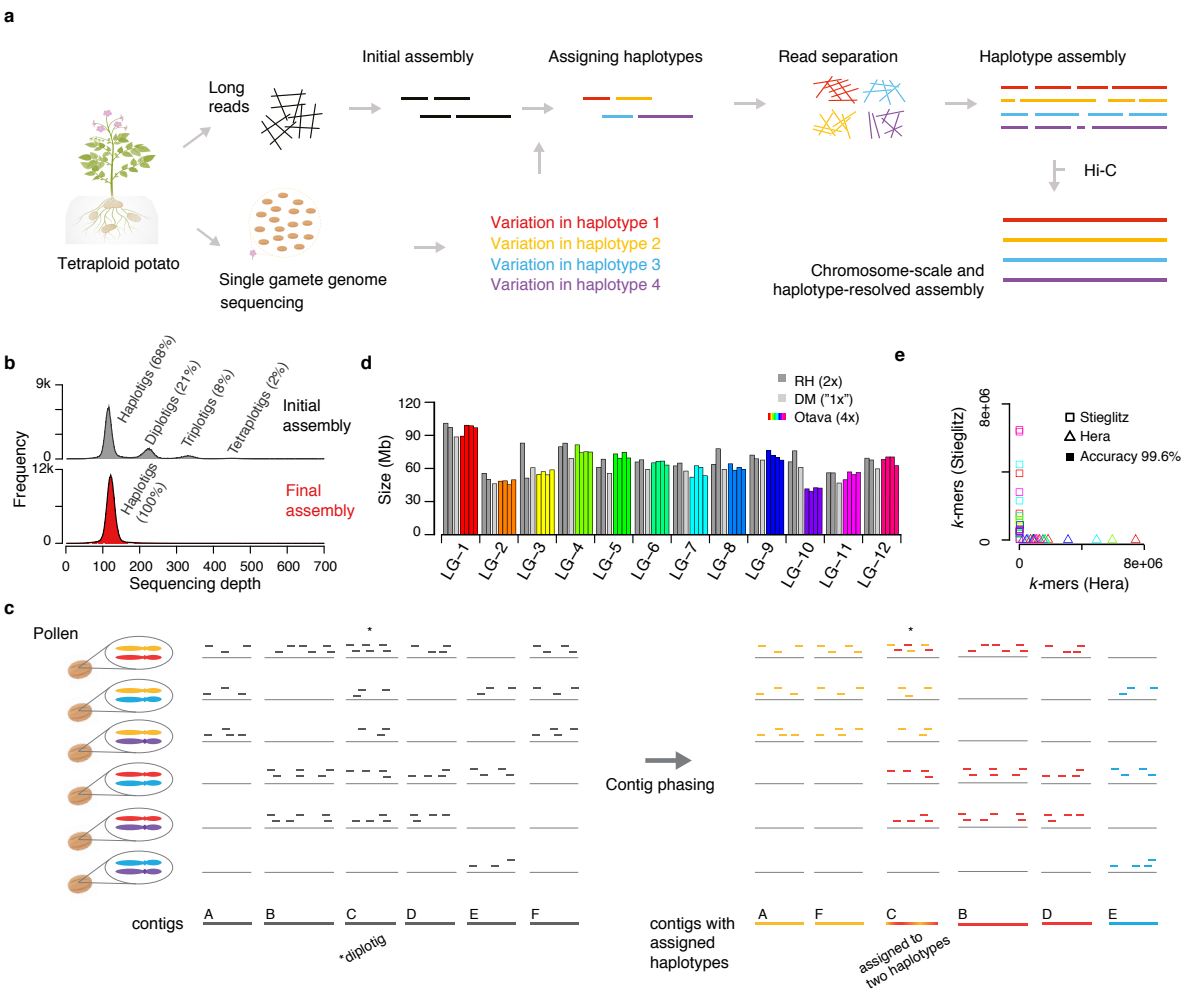

Figure 1. Haplotype-resolved assembly of an autotetraploid potato genome. a. Assembly strategy (gamete binning) for tetraploid genomes. Long reads are sequenced from somatic DNA and an initial contig-level assembly is generated. In addition, sequencing data of gamete genomes are generated. Genetic linkage enables grouping of the contig into clusters, which represent the individual haplotypes.

Long reads are assigned to haplotypes based on their similarity to the contigs. Each haplotype can be assembled separately and scaffolded to chromosome-scale using Hi-C. (The figure was created with help of BioRender.com.) **b.** Histogram of sequencing depth within 10 kb windows of the initial assembly (top) revealed the presence of haplotigs (68.3%), diplotigs (21.4%), triplotigs (7.9%) and tetraplotigs (2.0%). As a comparison, only one major peak was observed (with increased frequency) in the final assembly (bottom). **c.** Linkage grouping. Presence/absence patterns (PAP) at each coverage marker (50 kb region) are defined by the absence or presence of corresponding sequencing reads from each of the pollen genomes. For instance, the PAP of contig A is “111000”, where “1” refers to pollen genomes with reads that align to the contig and “0” refers to pollen genomes without such reads. PAPs of coverage markers A and F are highly correlated and can be grouped as {A, F}. Similarly, marker B and D are grouped as {B, D}, while coverage marker E remains ungrouped as {E}. The diplotig coverage marker C shows highest correlations to {A, F} and {B, D} as compared to {E}, and therefore extends these two larger clusters. Final result are the three clusters {A, C, F}, {B, C, D} and {E}. **d**. Assembly sizes of the haplotypes, which were highly consistent to the *DM*[5] and *RH*[7] assemblies. **e**. *k*-mer based evaluation of the haplotyping accuracy. Each point represents one haplotype of one individual chromosome. The values on the x- and y-axes indicate the numbers of *k*-mers within the haplotype sequence that are unique to either of the parental genomes 'Hera' or 'Stieglitz'. Overall, 99.6% of the variation were correctly phased.

To test if gamete binning could be applied for the genome assembly of 'Otava', we sequenced the genomes from 717 pollen nuclei with Illumina short reads with an average sequence coverage of 0.18x (Fig. S4) and aligned each of the 717 read sets against the initial assembly. As defining a high-density SNP list can be difficult in a highly heterozygous autotetraploid genome, we defined “coverage markers” (using average alignment depth in 50 kb windows) to assess if a genomic region was present in a pollen genome or not (Methods).

A coverage marker will be covered by reads if one of the two haplotypes of a pollen carries the region of the coverage marker. With this, we could assess the presence/absence pattern (PAP) of a coverage marker across all the 717 pollen genomes (Fig.1c). Closely linked markers featured highly similar PAPs, as most pollen genomes carried the same pair of haplotypes at two neighboring loci. Occasionally, recombination breakpoints, which are integrated into the pollen genomes during meiosis, change the haplotype within a pollen genome, and thereby slightly change the PAPs along the chromosome. However, as recombination is generally rare, closely linked coverage markers still feature highly correlated PAPs. We therefore could use the similarities between the PAPs to cluster the contigs into 48

121 groups representing the four haplotypes of all 12 chromosomes (Fig. S5-6). Haplotigs were
122 assigned to single clusters. Diplotigs, triplotigs and tetraplotigs represented multiple
123 haplotypes and were therefore assigned to two, three or four of the clusters (Methods).

124 Once the contigs were assigned to haplotypes, also the PacBio HiFi reads could be
125 assigned to these haplotypes based on their alignments against the contigs. Reads aligned to
126 diplotigs, triplotigs or tetraplotigs were randomly assigned to one of the respective haplotypes.
127 With this, more than 99.9% of the non-organellar PacBio HiFi reads could be assigned to one
128 of the 48 read sets (Fig. S7; Methods). Assembling the read sets using *hifiasm* resulted in 48
129 haplotype-resolved assemblies with an average N50 of 7.1 Mb and a total size of 3.1 Gb (92%
130 of the tetraploid genome). Finally, we used Hi-C short read data (130x per haplotype) to
131 scaffold the contigs of each assembly to a chromosome-scale, haplotype-resolved assembly
132 (Fig. S8; Methods). Comparison of the full assembly to whole genome sequencing short reads
133 of 'Otava' using *Merqury*[20] revealed very high base accuracy (QV > 51.7) and completeness
134 (97.3%) of the 'Otava' genome (Methods).

135 The sizes of the four haplotypes of each chromosome were highly consistent to each
136 other as well as to those of the *DM* and *RH* assemblies[4-7] except for the consistently shorter
137 assemblies of LG10, which indicated the presence of large-scale chromosomal
138 rearrangements between different cultivars, similar to those previously described[21] (Fig. 1d).
139 Apart from the LG10 differences, the 'Otava' assembly was in high synteny to the DM reference
140 sequence suggesting that also the structure of the chromosomes was assembled correctly
141 (Fig. S9-10). To evaluate the haplotyping accuracy of the tetraploid assembly in more depth,
142 we sequenced the parental cultivars of 'Otava', called 'Stieglitz' and 'Hera', with Illumina short
143 reads at 10x coverage per haplotype, as each of the chromosomes was either inherited from
144 'Stieglitz' or from 'Hera'. Comparing the *k*-mers, which are specific to one of the parental
145 genomes with each of the 48 chromosome assemblies, we found that each chromosome
146 included almost exclusively *k*-mers from one but not the other parent implying a haplotyping
147 accuracy of 99.6% (Fig. 1e; Methods).

148 Integrating *ab initio* predictions, protein and RNA-seq read[4-7] alignments, we annotated
149 152,855 gene models across four haplotypes, with an overall *BUSCO*[22] completeness score
150 of 97.3%, which is highly comparable to the annotations of the *RH* and *DM* assemblies[5,7](Data
151 S2-3; Methods). In addition, we found comparable amounts of various different types of non-
152 coding RNA for all haplotype genomes, which in total accounted for 33.9 Mb across the entire
153 genome (Data S4). Repetitive sequences made up 66% of the assembly with LTR
154 retrotransposons as the most abundant class and rDNA clusters of up to 600 kb in size, which
155 were assembled without any gaps (Data S5-6; Methods). The distribution of genes and repeats
156 along the chromosome followed the typical distribution of mono-centric plant genomes with
157 high gene and low repeat densities at the distal parts of the chromosome, while in the peri-
158 centromeric regions the gene densities were low and the repeat densities were high (Fig. 2).

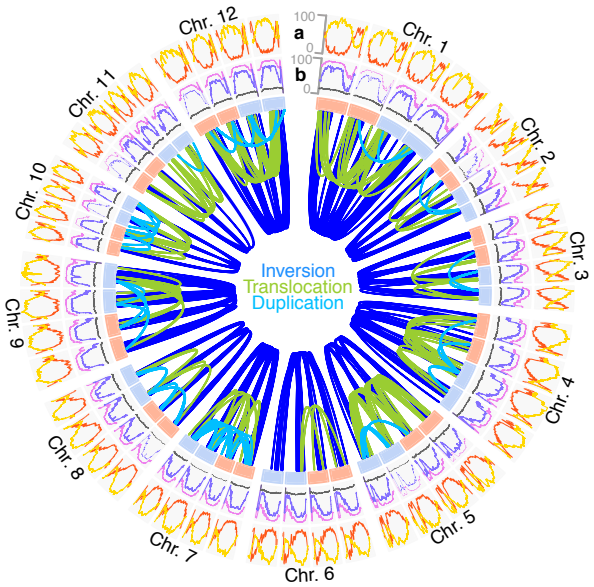

159
160 **Figure 2. The genomic features of the autotetraploid potato genome. a**. Gene density (number of
161 genes per Mb; red) and percentage of transposable element-related sequence (yellow) within 2 Mb
162 windows along the four haplotypes of each of the 12 chromosomes. **b**. Landscapes of methylation in
163 CG (purple), CHG (blue), CHH (gray) context within 2 Mb windows. The links in the center show over
164 600 structural rearrangements larger than 100 kb found between the four haplotypes of each
165 chromosome. Light blue and red box refer to the maternally and paternally inherited chromosomes.

166 **The genomic footprints of inbreeding**

167 A histogram of sequence differences within 10kb windows between the haplotypes
168 revealed two separated peaks implying the presence of highly similar as well as highly different

169 regions (Fig. 3a). The divergent regions included 1 SNP per 60 bp on average, while the
170 remaining 50% of the regions were almost without any differences (Fig. 3a). This extreme
171 similarity between some of the haplotypes suggested that they were recently inherited from a
172 common ancestor. In fact, the pedigree of many of the cultivated potatoes, including 'Otava',
173 contain cultivars that occur more than once in their ancestry[23,24] (Fig. S1). Common ancestors
174 in different lineages of the pedigree leads to inbreeding and results in regions which are
175 identical-by-descent (IBD) between their haplotypes (Fig. 3b-c; Fig. S11-22; Methods). The
176 IBD blocks almost perfectly matched the collapsed regions in the initial assembly explaining
177 the high degree of unresolved regions. To exclude any potential artefacts, we screened the
178 IBD blocks for collapsed variation (using pseudo-heterozygous variation in read alignments
179 against the assembly) and found that a maximum of 1 SNP in 72 kb could have been missed
180 (Data S7), reassuring that highly similar IBD regions do exist in the genome.

181 Overall, almost 50% of the tetraploid genome of 'Otava' were included in IBD blocks
182 and were shared by either two, three or in rare cases even by four haplotypes (Fig. 3b-d).
183 Individual IBD blocks varied in size and reached up to 41.6 Mb, while IBD blocks in the peri-
184 centromeres were significantly larger as compared to the IBD blocks in the distal parts of the
185 chromosomes (Fig. S11-23). Even though it is possible that long IDB blocks were recently
186 introduced and were not broken up by meiotic recombination yet, it is more likely that these
187 extremely long IBD blocks exist due to local suppression of meiotic recombination in the peri-
188 centromeres (Fig. 3c). Using the accumulated mutation rates in the IBD blocks as an estimate
189 of their age showed that long IBD blocks weren't younger as compared to short IBD blocks
190 (Fig. S23b).

191 **Extreme haplotype differences and their influence on genes**

192 The highly similar IBD blocks were contrasted by high levels of structural
193 rearrangements between the non-shared regions of the genome (Fig. 3; Fig. S11-22;
194 Methods). Inversions, duplications, and translocations made up 3.8% to 42.9% of each of the
195 haplotypes (or 19.3% of the genome) depending on the abundance of IDB blocks in the
196 respective haplotypes. Duplications and translocations were highly enriched for Gypsy and

197 Copia retrotransposons near their breakpoints suggesting their dynamic contribution to
198 genome diversification as it was described for other plant genomes before[25], while inversions
199 were not enriched for transposable elements (Fig. 3d; Fig. S24; Data S8).

200 Excluding IBD blocks, structural rearrangements made up 15.0% to 65.8% of each
201 chromosome. In addition, each haplotype included 11.0% to 42.5% of unique sequence that
202 could not be aligned to any of the other haplotypes (Fig. 3d). This amount of structural variation
203 and haplotype-specific sequence was much higher than what has been reported for any other
204 crop species so far, supporting earlier suggestions that genomic introgressions from wild
205 relatives were part of the domestication history of potato[26].

206 Overall, we found 661 structural variations longer than 100 kb which all were supported
207 by the contiguity of the assembled contigs or Hi-C contact signals, including 220 duplications,
208 207 translocations and 234 inversions (Fig. 2; Fig. S8,11-22,25; Data S9). While comparable
209 in number, inversions were much larger than the other types of rearrangements and reached
210 sizes of up to 12.4 Mb (Fig. 3e-f). Although these large inversions were mostly located in the
211 peri-centromeric regions where genes occur at low density, they still harbored nearly 5% of all
212 genes (7,958 out of 152,855). Meiotic crossover events from the pollen genomes were virtually
213 absent in inversions, indicating that these regions are likely to introduce large segregating
214 haplotypes among cultivated potato (Fig. 3c).

215 Pairwise allelic divergence of the genes ranged from 0 to 140 differences per kb and
216 included identical as well as divergent alleles. The average pairwise difference of the divergent
217 alleles was 18 differences per kb (Fig. 4a) and only 53.6% of the genes were present in all four
218 haplotypes. The remaining 46.4% of the genes were present in three (20.0%), two (15.9%) or
219 even only one (10.5%) of the haplotypes (Fig. 4b) with an average of 3.2 copies per gene. In
220 addition, the coding sequences of some of these copies were identical to each other. For
221 example, only 3,066 (15.4%) of the genes with four copies also featured four distinct alleles.
222 In consequence, even though each gene featured 3.2 copies on average, there were only 1.9
223 distinct alleles per gene (Fig. 4b).

While it was expected to find identical gene alleles within the IBD blocks, only ~45% of the identical gene alleles were actually within shared regions. To test if the high number of identical alleles between the otherwise different haplotypes was indicative of selection, we tested whether these genes were enriched for specific functions. This revealed a significant enrichment for genes with GO terms involving photosynthesis, chlorophyll binding and translation (Fig. 4c) suggesting a selection-induced reduction of allelic diversity through the optimization of plant performance.

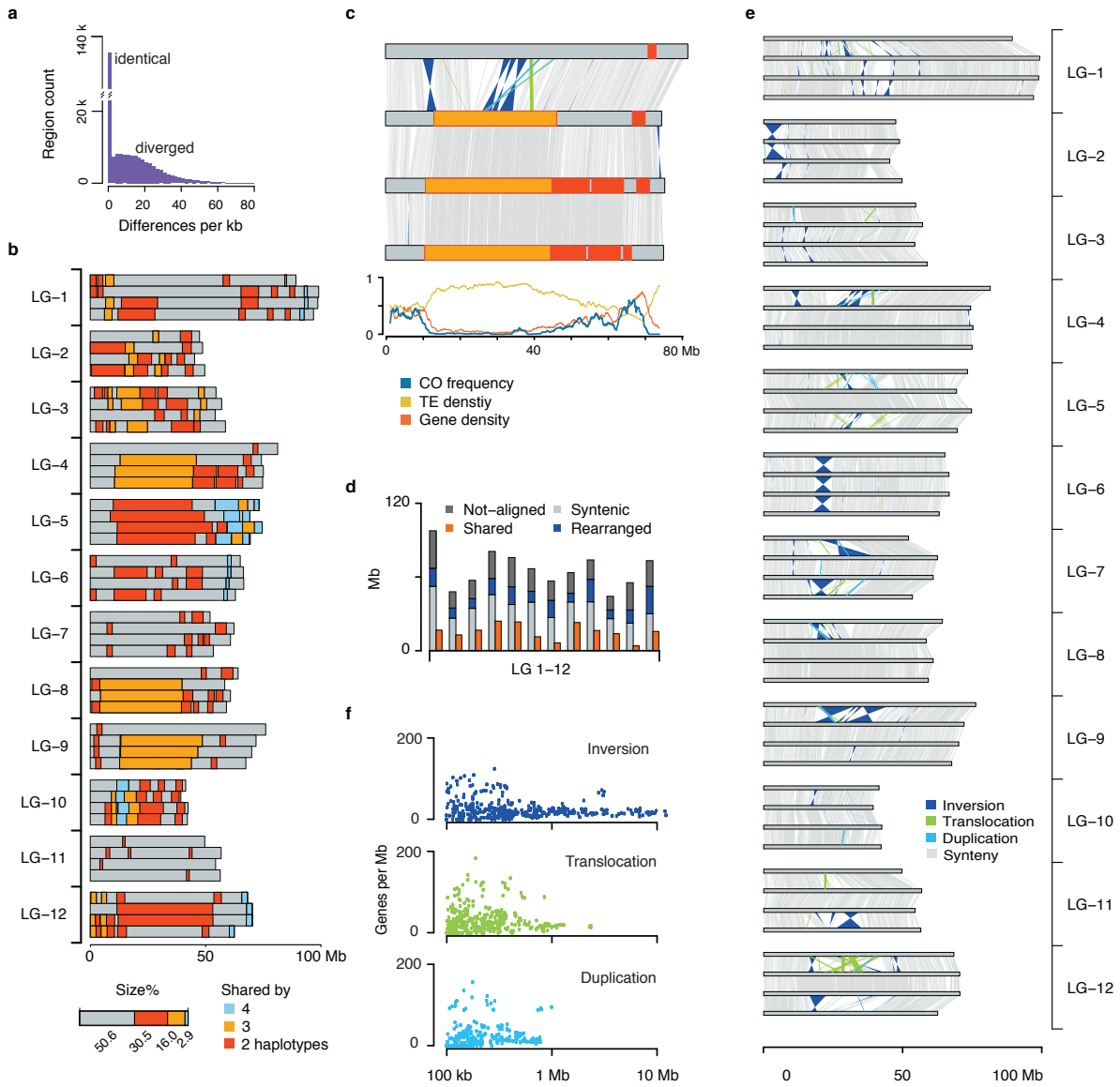

Figure 3. In-depth haplotype analysis of the tetraploid genome. a. SNP density as observed in pairwise comparisons between the haplotypes revealed two separated peaks. The high abundance of highly similar/identical regions suggested the existence of identical-by-descent (IBD) blocks. **b.** IBD blocks (minimum size: 1 Mb) across the genome. Regions shared by two, three or four haplotypes are

236 colored in red, orange or blue. **c.** A zoom-in on the IBD blocks and structural rearrangements of LG-4.
237 Large IBD blocks were more likely to occur in peri-centromeric regions with low gene, but high TE
238 content and suppressed meiotic recombination. (Colors as defined in **b** and **e**) **d.** Average alignment
239 statistics and structural rearrangements in each chromosome. **e.** Structural rearrangements between
240 the four haplotypes of each chromosome. **f.** Correlation of the individual size of 220 duplications, 207
241 translocations and 234 inversions with the respective gene density.

242 The low number of distinct alleles per gene and a selection-induced reduction of allelic
243 difference also implied that the tetraploid nature of the genome is not a necessary feature of
244 the high performance of potato in different environments. However, transforming potato into a
245 diploid suffers from the random distribution of the non-functional alleles throughout the
246 individual haplotypes implying that any ploidy reduction would lead to a significant gene loss**.**
247 In fact, the *BUSCO* score (indicating completeness) of the annotations of the individual
248 haplotypes was 89.5% on average, while the score of all four haplotypes combined was 97.3%
249 (Data S3) evidencing that the individual haplotypes lack genes which are present elsewhere
250 in the genome. Likewise, the doubled-monoploid *DM*[4,5] and the diploid *RH*[7] genomes, which
251 both were derived from tetraploid cultivars, feature 5,901 (15.4%) or 3,245 (8.5%), respectively,
252 less genes as compared to the tetraploid genome. The gene family with highest percentage of
253 genes with presence/absence variation (45.4%; 316 out of 696 genes) were the NLR
254 resistance genes (Data S10), which are known for their high intraspecies variability[27,28].

255 To investigate how genes are expressed in this tetraploid genome, we sequenced 367
256 million read pairs of the 'Otava' leaf transcriptome in three replicates (Data S1; Methods). The
257 four haplotype genomes contributed highly similar amounts of RNA, suggesting that none of
258 the haplotypes was dominant (Fig. 4d; Fig. S26), which is similar to observations in another
259 autoploid species[15]. Comparable to earlier analyses on the effects of CNVs on gene
260 expression[29], the number of allelic copies also impacted on gene expression. Genes with more
261 allelic copies showed a significantly increased gene expression as compared to genes with
262 fewer allelic copies (Fig. 4e). Although gene expression of the four haplotype genomes were
263 comparable at genome scale, 10.9% of the genes with four allelic copies featured significant
264 expression differences between the individual alleles (Fig. 4f).

To understand more about the regulation of allele-specific expression, we sequenced the DNA methylome of 'Otava' using enzymatic methylome sequencing with three replicates, each with 277 million read pairs (Data S1; Methods). Overall, we found that DNA methylation was consistent across all haplotypes while DNA methylation levels in IBD blocks were slightly higher as compared to the non-shared regions in the other haplotypes (Fig. 2; Fig. S27). Of the 1,219 genes with significant differences in the allele-specific expression, 304 genes were significantly correlated with the level of methylation at the up/downstream regions of these genes (Fig. 4g), suggesting that around 25% of the allele-specific expression are regulated through DNA methylation.

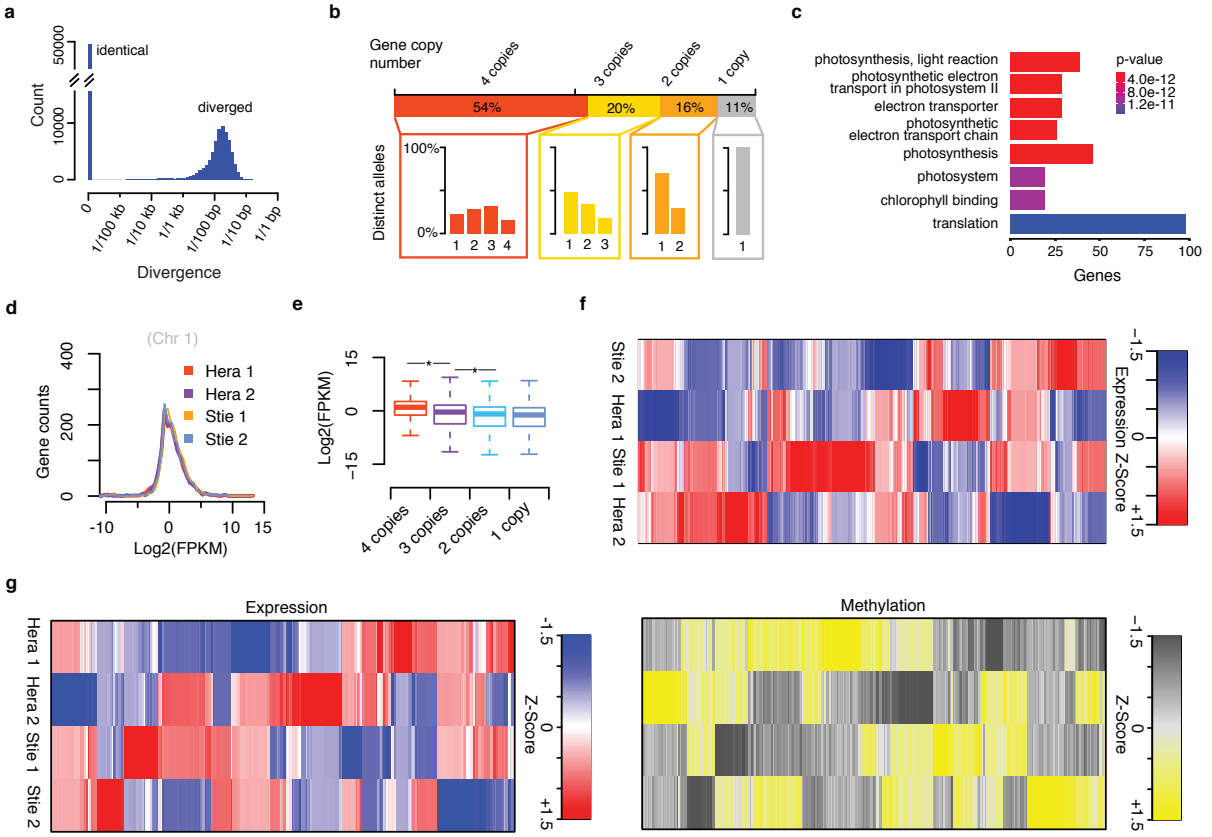

Figure 4. Impact of haplotype divergence on genes and their expression. a. Pair-wise evaluation of allelic divergence of genes. **b.** Presence/absence variations of genes. Overall, 53.6%, 20.0%, 15.9% or 10.5% of the genes showed four, three, two or one allelic copies/copy within the tetraploid genome with an average of 3.2 allelic copies per gene. Different configurations of divergent alleles were observed for the sets of genes with four, three or two copies, for instance, within the genes with four allelic copies, one (22.3%), two (29.8%), three (32.5%) or four (15.4%) divergent allele/s were observed. Overall, this led to an average of 1.9 distinct alleles per gene. **c.** GO enrichment analysis of genes with four identical alleles. **d**. Four haplotypes of chromosome 1 showed comparable amounts of expressed transcripts

283 (FPKM: fragments per kilobase per million reads; for chromosome 2-12 see Fig. S26). **e**. Genes with
284 more allelic copies are significantly higher expressed than those with fewer copies ('*': *t*-test, *p*-
285 value<0.01). **f**. Among the four haplotypes, 10.8% (1,219) of the 11,154 genes with four functional alleles
286 showed allele-specific expression (Data S11). **g**. Among those, allele-specific expression of 304 genes
287 was correlated with DNA methylation levels, which were measured in the 1 kb up- or downstream
288 regions surrounding the genes (Data S12).

289 **Discussions**

290 Here we reported the first haplotype-resolved assembly of an autotetraploid potato.
291 Leveraging high-quality, long reads and single-cell genotyping of diploid gametes, we were
292 able to reconstruct the sequences of all four haplotypes. The sequence differences between
293 the haplotypes were much higher as compared to the differences commonly found within
294 species and were rather reminiscent of the differences found between species. This supports
295 earlier suggestions that the diverse haplotypes originated from introgressions from divergent
296 species during domestication[26].

297 The high level of sequence differences, however, was contrasted by widespread IBD
298 blocks, which were most likely introduced by related genotypes during breeding, even though
299 we cannot exclude that some of these blocks might have been formed via double reduction
300 during meiosis[30]. This similarity of the IBD blocks was the reason for the abundant collapsed
301 regions in the initial assembly. As these regions were almost identical, it was not possible to
302 assemble them from the sequence data alone. IBD blocks are a widespread phenomenon in
303 many crops or livestock in general, though the challenges associated with the high similarity
304 between haplotypes can be solved by using the power of genetics and analyzing individual
305 gamete genomes.

306 The abundance of IBD blocks, in addition to IBD-independent allele sharing, led to the
307 unexpected observation that the tetraploid genome only included 1.9 diverse allelic copies per
308 gene. This implied that the maximal allelic diversity that could be included in the tetraploid
309 genome was not reached, even though the high yield and yield stability of potato is supposed
310 to be promoted by the effects of heterosis, which itself is based on non-additive interactions of
311 diverse alleles[31]. Whether the high abundance of shared alleles suggests that the effects of

312 heterosis could still be optimized by increasing the number of polymorphic alleles or if this
313 indicates that the limits of heterosis were already reached remains to be seen.

314 Over the past years, considerable success has been made in re-domesticating potato
315 from a clonally-propagated, tetraploid crop into a seed-propagated, diploid crop to increase
316 reproduction rate, decrease costs in storage and transportation, and improve disease
317 control[2,32-34]. However, the random distribution of loss-of-function alleles in tetraploid potato
318 can lead to the accelerated manifestation of inbreeding depression in the diploid genomes,
319 when they are derived from tetraploids[7,35]. Haplotype-resolved assemblies of autotetraploids
320 like the one presented here have the potential to support the design of optimal haplotypes by
321 avoiding the combination of known incompatibility alleles[36]. Of course, this new possibility to
322 assemble autotetraploid genomes does not eliminate all breeding-related problems that result
323 from the tetraploid nature of potato. However, being able to reconstruct the four haplotypes of
324 cultivated potato is a breakthrough for modern genomics-assisted breeding strategies, and
325 ultimately has the power to increase the breeding success of potato in the future.

326 **Methods**

327 Plant material was grown at Max Planck Institute for Plant Breeding Research
328 (Cologne, Germany). The genome of 'Otava' was sequenced with PacBio HiFi Sequel II
329 platform with four SMRTcells. DNA extracted from individual pollen nuclei was prepared with
330 10x Genomics CNV kits and subsequently sequenced with Illumina sequencing. Barcodes (in
331 single cell sequencing) were corrected using *cellranger* (10x Genomics). Short/long reads
332 were aligned using *bowtie2*[37]/*minimap2*[38]. BAM, VCF file processing and sequencing depth
333 analysis were performed using *samtools*[39] and *bedtools*[40]. Linkage grouping was performed
334 using in-house developed code. PacBio sequence reads were assembled using *hifiasm*[19], and
335 genome annotation was performed following a previous pipeline[9]. Structural variations were
336 identified using *SyRI*[41] based on *minimap2* genome alignments. Expression analysis was
337 performed following the literature[42]. Methylation calling was performed with *bismark* pipeline[43].
338 More details and other related methods are provided in the Supplementary Information.

339 **References**

340 1. The Food and Agriculture Organization (FAO). *http://www.fao.org/faostat/en/#data/QV*
341 (2021).
342 2. S. H. Jansky et al. Reinventing potato as a diploid inbred line-based crop. *Crop Sci.* **56**,
343 1412-1422 (2016).
344 3. D.S. Douches, D. Maas, K. Jastrzebski, R.W. Chase. Assessment of Potato Breeding
345 Progress in the USA over the Last Century. *Crop Sci*. **36**,1544-1552 (1996).
346 4. The Potato Genome Sequencing Consortium. Genome sequence and analysis of the tuber
347 crop potato. *Nature* **475**, 189-195 (2011).
348 5. G.M. Pham, J.P. Hamilton *et al*. Construction of a chromosome-scale long-read reference
349 genome assembly for potato. *GigaScience* **9**, 1-11 (2020).
350 6. C.D. Hirsch, J.P. Hamilton, K.L. Childs, J. Cepela, E. Crisovan, et al. (2014), Spud DB: A
351 Resource for Mining Sequences, Genotypes, and Phenotypes to Accelerate Potato
352 Breeding. *The Plant Genome* **7**, plantgenome2013.12.0042 (2014).
353 7. Q. Zhou, D. Tang *et al*. Haplotype-resolved genome analyses of a heterozygous diploid
354 potato. *Nat. Genet.* **52**, 1018-1023 (2020).
355 8. S. Koren, A. Rhie *et al*. De novo assembly of haplotype-resolved genomes with trio binning.
356 *Nat. Biotechnol.* **36**, 1174-1182 (2018).
357 9. J.A. Campoy, H. Sun *et al*. *Gamete binning*: chromosome-level and haplotype-resolved
358 genome assembly enabled by high-throughput single-cell sequencing of gamete genomes.
359 *Genome Biol.* **21**, 306 (2020).
360 10. R. Li, H. Qu *et al*. Inference of chromosome-length haplotypes using genomic data of three
361 or a few more single gametes. *Mol Biol Evol.* **37**, 3684-3698 (2020).
362 11. E.F. Kirkness *et al*. Sequencing of isolated sperm cells for direct haplotyping of a human
363 genome. *Genome Res.* **23**, 826-832 (2013).
364 12. D. Shi, J. Wu, H. Tang, H. Yin *et al*. Single-pollen-cell sequencing for gamete-based
365 phased diploid genome assembly in plants. *Genome Res.* **29**, 1889-1899 (2019).
366 13. C. Zhou, *et al*. Assembly of whole-chromosome pseudomolecules for polyploid plant

367 genomes using outbred mapping populations. *Nat. Genet*. **52**, 1256-1264 (2020).
368 14. S. Garg, *et al.* Chromosome-scale, haplotype-resolved assembly of human genomes. *Nat.*
369 *Biotechnol.* (2020).
370 15. J. Zhang, X. Zhang, H. Tang, Q. Zhang *et al*. Allele-defined genome of the autopolyploid
371 sugarcane *Saccharum spontaneum* L. *Nat. Genet.* **50**, 1565-1573 (2018).
372 16. H. Chen, Y. Zeng, Y. Yang, L. Huang, B. Tang, H. Zhang. et al. Allele-aware chromosome-
373 level genome assembly and efficient transgene-free genome editing for the autotetraploid
374 cultivated alfalfa. *Nat Commun* **11**, *2494* (2020).
375 17. X. Zhang, S. Zhang, Q. Zhao, R. Ming, H. Tang. Assembly of allele-aware, chromosomal-
376 scale autopolyploid genomes based on Hi-C data. *Nat. Plants* **5**, 833-845 (2019).
377 18. G. Linsmith *et al*. Pseudo-chromosome-length genome assembly of a double haploid
378 "*Bartlett*" pear (*Pyrus communis L.*). *GigaScience* **8**, 1-17 (2019).
379 19. H. Cheng, G.T. Concepcion, X. Feng, H. Zhang, H. Li. Haplotype-resolved de novo
380 assembly with phased assembly graphs. *Nat Methods* **18**, 170-175 (2021).
381 20. A. Rhie, B.P. Walenz, S. Koren, A.M. Phillippy. *Merqury*: reference-free quality,
382 completeness, and phasing assessment for genome assemblies. *Genome Biol* **21**, 1-27
383 (2020).
384 21. L. Comai, K. Amundson, B. Ordonez, X. Zhao, G. Tomaz Braz, J. Jiang, I. Henry. LD-CNV:
385 rapid and simple discovery of chromosomal translocations using linkage disequilibrium
386 between copy number variable loci. Preprint at Biorxiv (2021).
387 22. F.A. Simão and R.M. Waterhouse *et al*. *BUSCO*: Assessing genome assembly and
388 annotation completeness with single-copy orthologs. *Bioinformatics* **31**, 3210-3212 (2015).
389 23. R.C.B. Hutten and R.van Berloo. An online potato pedigree database. URL:
390 http://www.plantbreeding.wur.nl/PotatoPedigree/ (2001).
391 24. R.van Berloo, R.C.B. Hutten, H.J.van Eck, and R.G.F Visser. An online potato pedigree
392 database resource. *Potato research* **50**, 45-57 (2007).
393 25. E.M. Willing, V. Rawat, T. Mandáková et al. Genome expansion of *Arabis alpina* linked with
394 retrotransposition and reduced symmetric DNA methylation. *Nature Plants* **1**, 14023

395 (2015).
396 26. Ma.A. Hardigan, F.P.E. Laimbeer, L. Newton, E. Crisovan, J.P. Hamilton, B. Vaillancourt
397 et al. Genome diversity of tuber-bearing Solanum uncovers complex evolutionary history
398 and targets of domestication in the cultivated potato. *Proc Natl Acad Sci U S A* **114**, E9999-
399 E10008 (2017). doi: 10.1073/pnas.1714380114.
400 27. A.L. Van de Weyer, F. Monteiro, O.J. Furzer, et al. A Species-Wide Inventory of NLR
401 Genes and Alleles in Arabidopsis thaliana. *Cell*. **178**, 1260-1272 (2019).
402 28. K. Seong, E. Seo, K. Witek, M. Li, B. Staskawicz. Evolution of NLR resistance genes with
403 noncanonical N-terminal domains in wild tomato species. *New Phytol.* **227**, 1530-1543
404 (2020).
405 29. G.M. Pham, L. Newton, K. Wiegert-Rininger, B. Vaillancourt, D.S. Douches, C.R. Buell.
406 Extensive genome heterogeneity leads to preferential allele expression and copy number-
407 dependent expression in cultivated potato. *Plant J*. **92**, 624-637 (2017).
408 30. P.M. Bourke, R.E. Voorrips, R.G. Visser, C. Maliepaard. The double-reduction landscape
409 in tetraploid potato as revealed by a high-density linkage map. *Genetics*, 201:853-863
410 (2015).
411 31. J. Muthoni, H. Shimelis, R. Melis. Production of hybrid potatoes: Are heterozygosity and
412 ploidy levels important? *Australian Journal of Crop Science* **13**, 687-694 (2019).
413 32. P. Lindhout. *et al*. Towards F1 Hybrid Seed Potato Breeding. *Potato Res.* **54**, 301-312
414 (2011).
415 33. M. Ye, Z. Peng et al. Generation of self-compatible diploid potato by knockout of S-RNase.
416 *Nature Plants* **4**, 651-654 (2018).
417 34. Y. Li, G. Li, C. Li, D. Qu., S. Huang. Prospects of diploid hybrid breeding in potato. *Chin.*
418 *Potato J.* **27**, 96-99 (2013).
419 35. C. Zhang, P. Wang, D. Tang et al. The genetic basis of inbreeding depression in potato.
420 *Nat Genet.* **51**, 374-378 (2019).
421 36. Q. Lian, D. Tang, Z. Bai, J. Qi, F. Lu, S. Huang, C. Zhang. Acquisition of deleterious
422 mutations during potato polyploidization. *J Integr Plant Biol.* **61**, 7-11 (2019).

423 37. B. Langmead, S.L. Salzberg. Fast gapped-read alignment with *Bowtie* 2. *Nature methods*
424 **9**, 357-359 (2012).
425 38. H. Li. *Minimap2*: Pairwise alignment for nucleotide sequences. *Bioinformatics* **34**(18),
426 3094-100 (2018).
427 39. H. Li. et al. The Sequence Alignment/Map format and SAMtools. *Bioinformatics* **25**, 2078-
428 2079 (2009).
429 40. A.R. Quinlan, I.M. Hall. *BEDTools*: A flexible suite of utilities for comparing genomic
430 features. *Bioinformatics* **26**, 841-842 (2010).
431 41. M. Goel, H. Sun, W.B. Jiao, K. Schneeberger. *SyRI*: finding genomic rearrangements and
432 local sequence differences from whole-genome assemblies. *Genome Biol.* **20**, 1-13 (2019).
433 42. C.W. Law, M. Alhamdoosh, S. Su, X. Dong, L. Tian et al. RNA-seq analysis is easy as 1-
434 2-3 with limma, Glimma and edgeR. *F1000Research* **5**, ISCB Comm J-1408 (2016).
435 43. F. Krueger, S.R. Andrews. *Bismark*: a flexible aligner and methylation caller for Bisulfite-
436 Seq applications. *Bioinformatics* **27**, 1571-2 (2011).

Acknowledgements

The authors would like to thank Christiane Gebhardt (MPI-PZ, Cologne, Germany) and Benjamin Stich (HHU, Düsseldorf, Germany) for helpful discussions, Birgit Walkemeier and Christine Sänger (both MPI-PZ, Cologne, Germany) for plant cultivation, Christine Brandt and Klaus J. Dehmer (both IPK, Groß Lüsewitz, Germany) for providing material, Pádraic J. Flood (WUR, Wageningen, The Netherlands) for comments on the manuscript as well as Saurabh Pophaly (MPI-PZ, Cologne, Germany) for enthusiastic help in data management. We are very grateful to John Hamilton and C. Robin Buell (both University of Georgia, Georgia, USA) for integrating the 'Otava' assembly into Spud DB[6].

Funding

This work was funded by Deutsche Forschungsgemeinschaft (DFG, German Research Foundation) under Germany´s Excellence Strategy – EXC 2048/1– 390686111 (K.S.), and European Research Council (ERC) Grant "INTERACT" (802629) (K.S.). J.A.C was supported by Humboldt Research Fellowship for "Experienced Researchers" (Alexander von Humboldt Foundation) (J.A.C.), Marie Skłodowska-Curie Individual Fellowship PrunMut (789673).

Author contributions

H.S. and K.S. developed the project. J.A.C., H.S. and K.S. coordinated the generation of data with K.K., K.F-D., C.K. and B.H.. H.S., W-B.J., and M.G. performed all data analysis. H.S. and K.S. wrote the manuscript with input from all authors. All authors read and approved the final manuscript.

Competing interests

The authors declare no competing interests.

Data and materials availability

High-throughput sequencing data analyzed in this project are available under NCBI BioProject: PRJNA751899. This Whole Genome Shotgun project (including assembly and annotation) has been deposited at DDBJ/ENA/GenBank under the accessions JAIVGA000000000, JAIVGB000000000, JAIVGC000000000 and JAIVGD000000000. The version described in this paper is version JAIVGA010000000, JAIVGB010000000,

465 JAIVGC010000000 and JAIVGD010000000. The genome assembly and gene annotation of
466 'Otava' are also available on Spud DB (http://spuddb.uga.edu/)[6]. Customed code and scripts
467 supporting this work are available at *github.com/schneeberger-lab/GameteBinning_tetraploid*.

Supplementary Information

Materials and Methods

Figs. S1 to S28

Data S1 to S12